

1 **Brain volumetric changes in the general population following the COVID-19 outbreak and**
2 **lockdown**

3 Tom Salomon¹, Adi Cohen^{1,2}, Gal Ben-Zvi^{1,2}, Rani Gera^{1,2,3}, Shiran Oren^{1,2}, Dana Roll¹, Gal
4 Rozic¹, Anastasia Saliy¹, Niv Tik^{2,4}, Galia Tsarfati⁵, Ido Tavor^{*2,4,6}, Tom Schonberg^{*1,2,6}, Yaniv
5 Assaf^{*1,2,6}

6 * corresponding authors equal contribution

7

- 8 1. School of Neurobiology, Biochemistry and Biophysics, Faculty of Life Science, Tel Aviv
9 University, Tel Aviv, Israel
- 10 2. Sagol School of Neuroscience, Tel Aviv University, Tel Aviv, Israel
- 11 3. School of Psychological Sciences, Tel Aviv University, Tel Aviv, Israel
12
- 13 4. Department of Anatomy and Anthropology, Faculty of Medicine, Tel Aviv University,
14 Tel Aviv, Israel
- 15 5. Division of Diagnostic Imaging, Sheba Medical Center, Tel-Hashomer, affiliated to the
16 Faculty of Medicine, Tel Aviv University, Tel Aviv, Israel
- 17 6. The Strauss Center for Computational Neuroimaging, Tel Aviv University, Tel Aviv,
18 Israel

19

20

21 **Abstract**

22 The COVID-19 outbreak introduced unprecedented health-risks, as well as pressure on the
23 financial, social, and psychological well-being due to the response to the outbreak¹⁻⁴. Here, we
24 examined the manifestations of the COVID-19 outbreak on the brain structure in the healthy
25 population, following the initial phase of the pandemic in Israel. We pre-registered our
26 hypothesis that the intense experience of the outbreak potentially induced stress-related brain
27 modifications⁵⁻⁸. Volumetric changes in $n = 50$ participants scanned before and after the
28 COVID-19 outbreak and lockdown, were compared with $n = 50$ control participants that were
29 scanned twice prior to the pandemic. The pandemic provided a rare opportunity to examine brain
30 plasticity in a natural experiment. We found volumetric increases in bilateral amygdalae,
31 putamen, and the anterior temporal cortices. Changes in the amygdalae diminished as time
32 elapsed from lockdown relief, suggesting that the intense experience associated with the
33 pandemic outbreak induced volumetric changes in brain regions commonly associated with
34 stress and anxiety⁹⁻¹¹.

35

36 **Main text**

37 Since early 2020, the world has been coping with the outbreak of the coronavirus disease 2019
38 (COVID-19) pandemic that has infected millions with devastating numbers of deaths globally.
39 As an initial response to the first wave of the outbreak, countries closed their borders and
40 implemented a series of ad-hoc laws and orders to restrict the spread of the disease. Countries
41 with major outbreaks such as China, Italy, and Spain enforced stringent restriction of movement
42 for a limited period, referred to here as 'lockdown'. Although lockdowns contributed to
43 restricting the health risks of the outbreak¹², they also had a negative impact on the social,

44 economic and psychological well-being of the general population, leading to one of the sharpest
45 declines in economic growth over the past decades^{1,2}. Lockdowns also led to high rates of stress
46 and anxiety which were attributed in large to the social and financial consequences of responding
47 to the health crisis⁴. It is now evident that the indirect consequences of the pandemic affected a
48 much larger proportion of the population, having an impact of no lesser gravity than the actual
49 health risks that were meant to be prevented^{3,13}.

50 In Israel, a strict lockdown period was issued from mid-March until the end of April. During its
51 peak, most unessential businesses were closed and civilians' movement for non-essential
52 destinations was restricted for a radius of 100 meters from their homes. Prior to COVID-19, the
53 country had experienced a period of peak economic prosperity¹⁴, which was interrupted by the
54 outbreak, leading to unprecedented unemployment rates (reaching nearly 30% of the work-force
55 in April 2020) and the collapse of several sectors such as aviation, tourism, and culture^{15,16}. The
56 outbreak period was characterized with acute uncertainty and increase in anxiety, regarding both
57 the health and socioeconomic effects of the pandemic¹⁷.

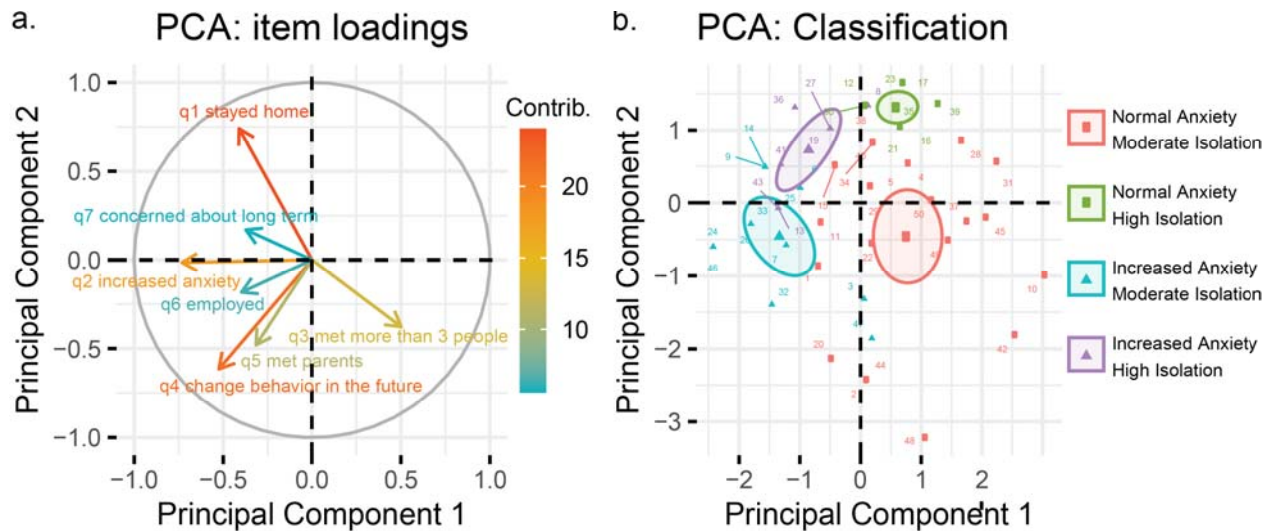
58 Over the past years several studies demonstrated brain plasticity detected using T1-weighted
59 magnetic resonance imaging (MRI)¹⁸⁻²⁰. The current work was initiated as a reaction to the
60 outbreak of COVID-19 in Israel, aimed to study the structural brain plasticity in the general
61 population following a real-life event of global scale. For this purpose, we examined $n = 50$ test
62 group participants that were scanned with T1-weighted MRI prior to the outbreak and returned
63 for a follow-up scan after the lockdown period. The structural changes of the study group (before
64 versus after the outbreak) were compared to those of $n = 50$ control participants who were
65 scanned twice before the COVID-19 outbreak. The unique circumstances imposed due to the

66 COVID-19 lockdown created rare settings for a natural experiment to examine the effect of a
67 real-world intense event on brain plasticity.

68 All participants were healthy, without a history of neurological or psychiatric disorders, did not
69 show COVID-19 symptoms, and were not diagnosed carrying the virus (see the methods section
70 for further demographic information). The hypotheses and general design of the current study
71 were pre-registered prior to the completion of data collection and were based on a small
72 independent pilot sample with $N = 16$ participants ($n = 8$ participants in each group). The data
73 and analysis codes are openly shared online (project page: <https://osf.io/wu37z/>; preregistration:
74 <https://osf.io/k6xhn/>).

75 Prior to their follow-up MRI scan session, we asked participants of the post-lockdown test group
76 to fill in a short questionnaire regarding the lockdown period (see methods). Of the participants
77 who agreed to reply, 79.6% reported they did not leave their home for non-essential needs,
78 38.8% indicated an increased feeling of anxiety following the lockdown, 79.6% met no more
79 than 3 people, 34.7% anticipated that their future behavior will change after the lockdown,
80 44.9% did not meet with their parents at all, 42.9% indicated that their employment status was
81 reduced to part-time or unemployment, 46.8% reported they were concerned about their personal
82 future well-being. In an exploratory principal component analysis (PCA), we found that two
83 principal components best explain the variability in the data, explaining together 42.58% of the
84 variance. The first component was highly loaded with increased feelings of anxiety, and the
85 second was related to items describing increased social isolation (Figure 1). These analyses (not
86 included in the pre-registration) indicate that the pandemic outbreak had a significant impact on
87 the social and psychological well-being of most participants in our study.

88



89

90 **Figure 1.** Principal component analysis of COVID-19 questionnaire.

91 A principal component analysis (PCA) of the responses to the questionnaire revealed two main
92 themes characterized the participants. **a.** An increased feeling of anxiety dominated the first
93 principal component (x-axis), while the three items relating to social distancing (staying at home,
94 meeting parents and meeting more than 3 people) contributed together to the second component
95 (y-axis). **b.** Visualization of participants dispersion across the two principal components and their
96 categorization into binary anxiety and isolation groups. High isolation was defined as directional
97 response to all three social-isolation items described above. Points represent individual
98 participants.

99

100 Based on our pilot study results and previous studies of stress-related morphological brain
101 changes⁵⁻⁸ we hypothesized that the focus of volumetric changes will be observed mainly in the
102 amygdalae. The anatomical data were used as input for deformation and surface-based
103 morphometry (SBM) analysis using the CAT12 toolbox (<http://www.neuro.uni-jena.de/cat/>,
104 University of Jena) for SPM12 (<http://www.fil.ion.ucl.ac.uk/spm/software/spm12/>, Wellcome
105 Trust Centre for Neuroimaging). The brain was segmented to 58 regions based on the cortical
106 and subcortical nuclei classifications of the Hammers atlas (Hammers et al., 2003). Following
107 surface reconstruction, each participant's individual gray matter volume was estimated for each
108 of the 58 anatomically defined regions of interest (ROIs). This procedure accounted for the
109 longitudinal nature of the data, performing the analysis on both scans simultaneously. To avoid
110 voxel-based multiple comparisons, we performed a region-based analysis (following surface

111 projection to the Hammer atlas) and corrected for multiple comparisons using the Benjamini-
112 Hochberg correction²¹ to control for false discovery rate (FDR; at $p < 0.05$ following correction).
113 Validation of this pipeline was performed using simulated data and by comparing the results with
114 other software (see methods).

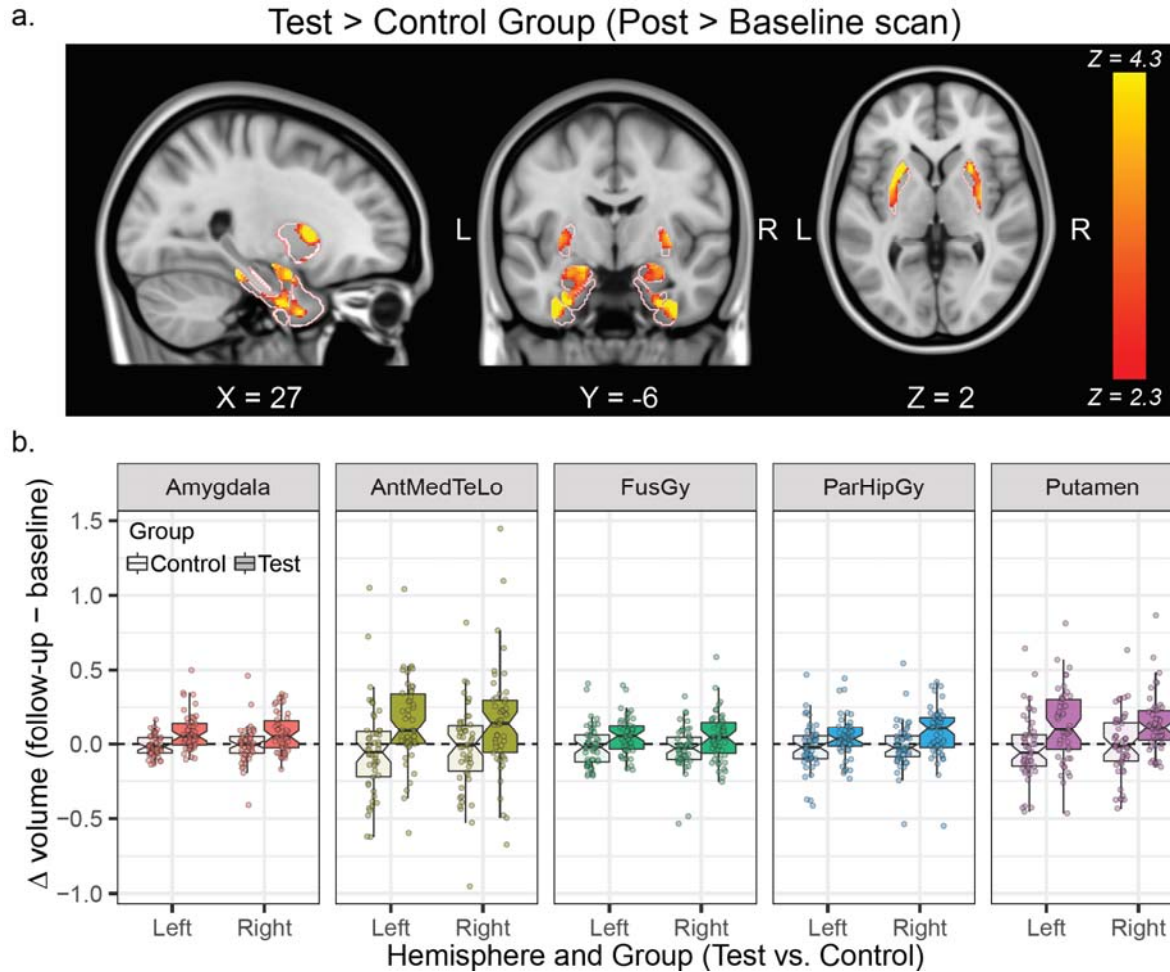
115 Using a linear mixed model, we examined volumetric changes, testing for regions with stronger
116 effects for the test group, compared to the control group. Examining an interaction effect of
117 session (baseline versus follow-up scans) and experimental group (test versus control) revealed
118 ten anatomical brain regions (composed of bilateral five unique regions in both hemispheres) in
119 which volumetric increases were observed uniquely for the test group (Table 1 and Figure 2).
120 Most prominently, as we expected and pre-registered, we found a robust effect in the bilateral
121 amygdalae. We also observed a significant effect bilaterally in the putamen, and in three
122 anatomical regions within the ventral anterior temporal cortex adjacent to each other, namely in
123 the medial part of the anterior temporal lobe, the fusiform gyrus, and the parahippocampal gyrus.

124 To examine the spatial distribution within significant ROIs, we performed an additional post-hoc
125 voxel-based analysis, which allowed us to visualize the changes within the significant ROIs
126 (Figure 2a). Examining the post-hoc voxel-based results revealed that volumetric changes
127 occurred throughout the entire surface of bilateral amygdalae, while in the putamen the effects
128 occurred mainly in the dorsal area. In the ventral anterior temporal cortices, large connected
129 clusters of volumetric change spanned throughout the three adjacent temporal ROIs, thus
130 suggesting that the three ROIs shared a similar origin. In all ROIs, we ensured that the significant
131 effect was apparent for the test group but not for the control group (see methods), suggesting that
132 the reported interaction effects originated from volumetric changes in the test group following
133 the COVID-19 outbreak and its related lockdown period (Figure 2b).

134 **Table 1. Surface based morphology analysis results**

Region	Hemi-sphere	Interaction estimate (95% CI)	Interaction <i>p</i> (FDR adj.)	Session estimate (95% CI) ^a	Session <i>p</i> (FDR adj.)
Amygdala	Left	0.09 [0.05, 0.13]	2.4E ⁻⁵ (0.001)	0.08 [0.05, 0.11]	9.8E ⁻⁶ (2.1E ⁻⁴)
	Right	0.08 [0.03, 0.13]	0.003 (0.030)	0.08 [0.05, 0.11]	1.6E ⁻⁵ (2.3E ⁻⁴)
Putamen	Left	0.19 [0.09, 0.29]	4.1E ⁻⁴ (0.006)	0.13 [0.06, 0.2]	4.0E ⁻⁴ (0.002)
	Right	0.17 [0.08, 0.26]	2.4E ⁻⁴ (0.005)	0.14 [0.08, 0.2]	1.1E ⁻⁵ (2.1E ⁻⁴)
Anterior temporal lobe (medial part)	Left	0.25 [0.12, 0.38]	1.8E ⁻⁴ (0.005)	0.15 [0.07, 0.23]	4.7E ⁻⁴ (0.003)
	Right	0.21 [0.07, 0.35]	0.004 (0.030)	0.15 [0.05, 0.25]	0.004 (0.023)
Parahippocampal gyrus	Left	0.09 [0.03, 0.15]	0.006 (0.035)	0.04 [0, 0.08]	0.029 (0.085)
	Right	0.11 [0.04, 0.18]	0.003 (0.030)	0.08 [0.03, 0.13]	0.002 (0.009)
Fusiform gyrus	Left	0.08 [0.03, 0.13]	0.007 (0.036)	0.06 [0.03, 0.09]	3.8E ⁻⁴ (0.003)
	Right	0.11 [0.04, 0.18]	0.002 (0.022)	0.05 [0, 0.1]	0.044 (0.111)

135 ^a Session estimate examined the effect of baseline versus follow-up scan in the post-lockdown
136 test group. This parameter was used to validate that the interaction effect observed between the
137 group stemmed from a robust effect in the test group (see methods).
138



139

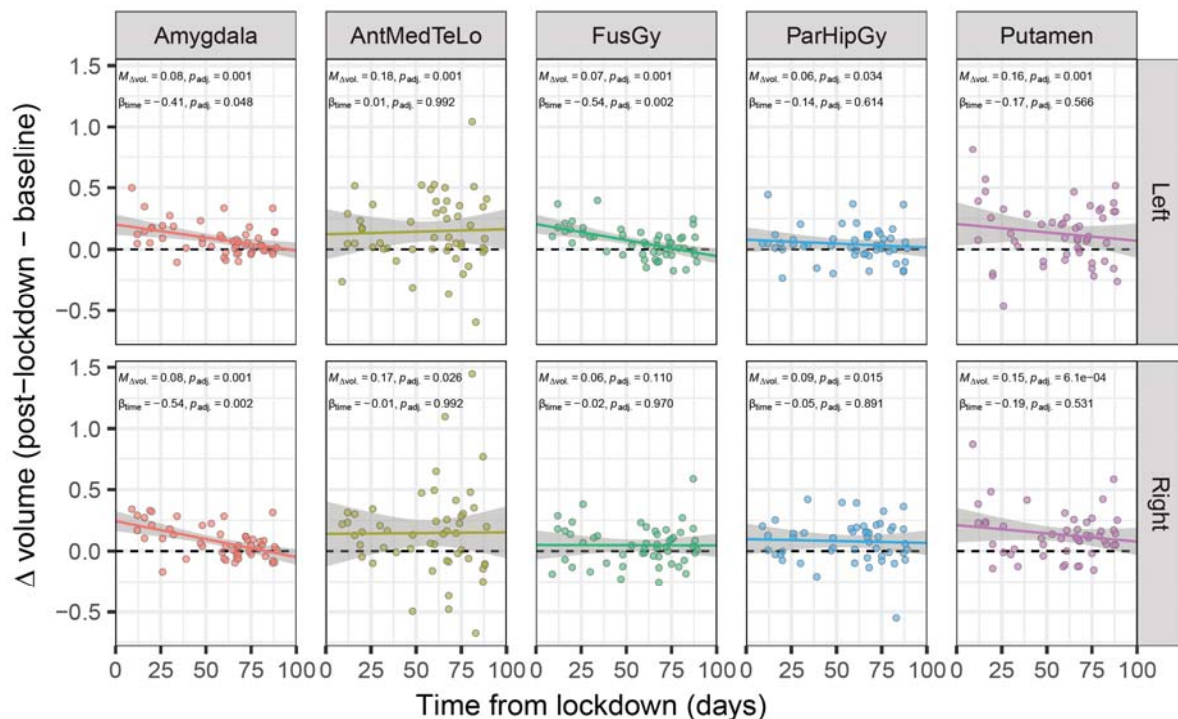
140 **Figure 2.** Volumetric changes results.

141 An interaction effect for time (baseline versus follow-up scan) and group (test versus control)
 142 was evaluated on segmented surfaces in an SBM analysis. Significant interaction effects were
 143 observed bilaterally in the amygdala and putamen ROIs, as well as in three ventral temporal
 144 cortical ROIs. **a.** To examine spatial patterns within the identified ROIs, a post-hoc voxel-based
 145 analysis was conducted within each ROI mask. Light red contours represent segmentation
 146 borders of the ROIs. **b.** Individual distribution of the results in the control group (light colors)
 147 and test group (dark colors). Box-plot center, hinges, and whiskers represent the median,
 148 quartiles, and from the hinges, respectively. A notch of represent an
 149 estimated 95% confidence interval for comparing medians. Dots represent individual
 150 participants. Abbreviated ROI names: AntMedTeLo = anterior temporal lobe (medial part);
 151 FusGy = fusiform gyrus, ParHipGy = Parahippocampal gyrus.

152

153 To evaluate and control for the effect of time between scans and time from lockdown, we
 154 included in the model two additional covariates - the time between scans (TBS; which was
 155 generally longer for the test group) and time following lockdown (TFL; see supplementary
 156 methods for more details). The two covariates were not correlated with each other in our test

157 group sample ($r = -0.106$, $t(48) = -0.74$, $p = 0.463$). Our reported regions demonstrated
 158 significant volumetric change above and beyond these covariates. After FDR correction, no
 159 region showed an effect of TBS. However, we did find a negative effect of TFL in the two
 160 amygdalae ROIs and the left fusiform gyrus, suggesting that the volumetric changes in these
 161 regions moderated as time following lockdown elapsed. Based on these results we estimated the
 162 time to decay as the estimated number of days from lockdown until volumetric changes returned
 163 to normal levels, similar to those of the control group (left amygdala: $\beta_{\text{TFL}} = -0.41$, $t(47) = -3.1$, p
 164 $= 0.003$, $p_{\text{adj.}} = 0.048$, time to decay = 95 days; right amygdala: $\beta_{\text{TFL}} = -0.54$, $t(47) = -4.38$, $p =$
 165 $6.7E^{-5}$, $p_{\text{adj.}} = 0.002$, time to decay = 83 days; left fusiform gyrus: $\beta_{\text{TFL}} = -0.54$, $t(47) = -4.44$, $p =$
 166 $5.5E^{-5}$, $p_{\text{adj.}} = 0.002$, time to decay = 82 days; Figure 3).



167

168 **Figure 3.** Time following lockdown effect on volumetric changes.

169 The time from lockdown relief until the follow-up scan session (TFL) was introduced as addition
 170 covariate to the model, revealing significant effect in the two amygdalae and left fusiform gyrus.
 171 Points represent individual participants in the post-lockdown test, p -values were FDR adjusted
 172 for multiple comparisons. Abbreviated ROIs: AntMedTeLo = anterior temporal lobe (medial
 173 part); FusGy = fusiform gyrus, ParHipGy = Parahippocampal gyrus.

174

175 Additional exploratory analyses examined the association of volumetric changes and the reported
176 experience during lockdown. We found no strong association between the two, as reported in the
177 supplementary results.

178 In conclusion, our study demonstrates that volumetric change patterns in the brain occurred
179 following the COVID-19 initial outbreak period and restrictions. Previous studies demonstrated
180 brain plasticity using T1-weighted MRI following planned interventions¹⁸⁻²⁰. The current work
181 uniquely demonstrates stark structural brain plasticity following a major real-life event.

182 Our findings show changes in gray matter in the amygdala, putamen and ventral anterior
183 temporal cortex. The changes in the amygdalae showed a temporal-dependent effect, related to
184 the time elapsed from lockdown but not the duration from the baseline scan. It should be noted
185 that although lockdown restrictions had initially reduced infection rates in Israel, just one month
186 after the lockdown was lifted, the number of infected cases started to rise again and reached
187 higher number of active infected cases by the end of data collection, compared with the peak
188 numbers during the actual lockdown period (approximately 2,000 daily new cases by the end of
189 July versus under 750 new daily cases during the peak of the lockdown period in April²², see
190 supplementary Figure 1). This suggests that the effects observed in the current study are less
191 likely to be attributed to the concrete health risks of COVID-19, but rather to the first wave of
192 the outbreak, characterized with perceived uncertainty.

193 The current study was in many aspects unplanned; thus we are left with only partial answers as
194 to which specific components of the COVID-19 outbreak led to the neural changes observed in
195 the healthy participants that took part in our study. The involvement of the amygdala may
196 suggest that stress and anxiety could be the source of the observed phenomenon, due to its well-
197 recorded functional and structural associations⁵⁻¹¹. Nevertheless, it is hard to draw clear

198 conclusions as many aspects of life have changed in this time period, and could have potentially
199 affected different regions in the brain – from limiting social interactions, increased financial
200 stress, changes in physical activity, work routine, and many more. The limited behavioral data
201 collected in the current study did not provide a strong connection to the imaging results, and thus
202 future work could try to better address the complex brain-behavioral associations in this real-life
203 experience. Nonetheless, our findings show healthy young adults, with no records of mental
204 health issues, were deeply affected by the outbreak of COVID-19. We suggest that policy makers
205 take into consideration the impact of their actions on the general well-being of the population
206 they seek to help, alongside the efficacy of disease prevention.

207

208 **Acknowledgements**

209 This work was supported by the Israeli Science Foundation granted to Yaniv Assaf (ISF
210 1314/15), Tom Schonberg (2004/15), and Ido Tavor (ISF 1603/18). Tom Salomon was supported
211 by the Nehemia Levtzion fellowship and the Fields-Rayant Minducate Learning Innovation
212 Research Center. We would also want to thank Dr. Daniel Barazany, the manager of the Strauss
213 MRI center, for his invaluable assistance throughout the study.

214

215 **Author contributions**

216 T.Sa. wrote the manuscript with Y.A, assisted with the study design and analyzed the data. Data
217 was collected by A.C., R.G, S.O, G.R., D.R, and A.S. Free-surfer analysis was made by G.B-Z.
218 N.T performed VBM validation analysis. G.T. provided support and medical supervision. I.T.,
219 T.Sc. and Y.A. conceived the study, wrote the manuscript and supervised the study. Y.A

220 performed the preprocessing and analysis of imaging data. All Author contributed intellectually
221 and reviewed the manuscript.

222

223 **Competing interests**

224 The authors declare no competing financial interests.

225

226 **References**

- 227 1. Zhang, D., Hu, M. & Ji, Q. Financial markets under the global pandemic of COVID-19.
228 *Financ. Res. Lett.* 101528 (2020). doi:10.1016/j.frl.2020.101528
- 229 2. Fernandes, N. Economic effects of coronavirus outbreak (COVID-19) on the world
230 economy Nuno Fernandes Full Professor of Finance IESE Business School Spain. *SSRN*
231 *Electron. Journal, ISSN 1556-5068, Elsevier BV, 0–29* (2020).
- 232 3. Gruber, J. *et al.* Mental health and clinical psychological science in the time of COVID-
233 19: Challenges, opportunities, and a call to action. *Am. Psychol.* (2020).
234 doi:<https://doi.org/10.1037/amp0000707>
- 235 4. Taylor, S. *et al.* COVID stress syndrome: Concept, structure, and correlates. *Depress.*
236 *Anxiety* 1–9 (2020). doi:10.1002/da.23071
- 237 5. Ganzel, B. L., Kim, P., Glover, G. H. & Temple, E. Resilience after 9/11: Multimodal
238 neuroimaging evidence for stress-related change in the healthy adult brain. *Neuroimage*
239 **40**, 788–795 (2008).
- 240 6. Hölzel, B. K. *et al.* Stress reduction correlates with structural changes in the amygdala.
241 *Soc. Cogn. Affect. Neurosci.* **5**, 11–17 (2009).
- 242 7. Rogers, M. A. *et al.* Smaller amygdala volume and reduced anterior cingulate gray matter
243 density associated with history of post-traumatic stress disorder. *Psychiatry Res. -*
244 *Neuroimaging* **174**, 210–216 (2009).
- 245 8. Schienle, A., Ebner, F. & Schäfer, A. Localized gray matter volume abnormalities in
246 generalized anxiety disorder. *Eur. Arch. Psychiatry Clin. Neurosci.* **261**, 303–307 (2011).
- 247 9. Stevens, J. S. *et al.* Amygdala Reactivity and Anterior Cingulate Habituation Predict
248 Posttraumatic Stress Disorder Symptom Maintenance After Acute Civilian Trauma. *Biol.*

- 249 *Psychiatry* **81**, 1023–1029 (2017).
- 250 10. Bryant, R. A. *et al.* Enhanced amygdala and medial prefrontal activation during
251 nonconscious processing of fear in posttraumatic stress disorder: An fMRI study. *Hum.*
252 *Brain Mapp.* **29**, 517–523 (2008).
- 253 11. Mochcovitch, M. D., Da Rocha Freire, R. C., Garcia, R. F. & Nardi, A. E. A systematic
254 review of fMRI studies in generalized anxiety disorder: Evaluating its neural and
255 cognitive basis. *J. Affect. Disord.* **167**, 336–342 (2014).
- 256 12. Vinceti, M. *et al.* Lockdown timing and efficacy in controlling COVID-19 using mobile
257 phone tracking. *EClinicalMedicine* (2020). doi:10.1016/j.eclinm.2020.100457
- 258 13. Qiu, J. *et al.* A nationwide survey of psychological distress among Chinese people in the
259 COVID-19 epidemic: Implications and policy recommendations. *Gen. Psychiatry* **33**, 1–4
260 (2020).
- 261 14. Bank of Israel Research Department. The Decline in Unemployment in Israel by
262 International Comparison. in *Bank of Israel Annual Report 2019* (2020).
- 263 15. Bank of Israel Research Department. *The unemployment rate and its definition during the*
264 *corona period.* (2020).
- 265 16. Bank of Israel Research Department. *Changes in credit card purchases as a result of the*
266 *corona crisis.* (2020).
- 267 17. Tzur Bitan, D. *et al.* Fear of COVID-19 scale: Psychometric characteristics, reliability and
268 validity in the Israeli population. *Psychiatry Res.* **289**, 113100 (2020).
- 269 18. Maguire, E. A. *et al.* Navigation-related structural change in the hippocampi of taxi
270 drivers. *Proc. Natl. Acad. Sci. U. S. A.* **97**, 4398–4403 (2000).
- 271 19. Jung, W. H. *et al.* Exploring the brains of Baduk (Go) experts: Gray matter morphometry,
272 resting-state functional connectivity, and graph theoretical analysis. *Front. Hum.*
273 *Neurosci.* **7**, 633 (2013).
- 274 20. Draganski, B. *et al.* Changes in grey matter induced by training. *Nature* **427**, 311–312
275 (2004).
- 276 21. Benjamini, Y. & Hochberg, Y. Controlling the False Discovery Rate: A Practical and
277 Powerful Approach to Multiple Testing. *J. R. Stat. Soc. Ser. B* **57**, 289–300 (1995).
- 278 22. Israel Ministry of Health. Coronavirus in israel - Overview (in Hebrew). (2020). Available
279 at: <https://datadashboard.health.gov.il/>. (Accessed: 31st August 2020)

- 280 23. Champely, S. *et al.* Package ‘pwr’: Basic Functions for Power Analysis. *CRAN Repos.*
281 (2018).
- 282 24. Manjón, J. V., Coupé, P., Martí-Bonmatí, L., Collins, D. L. & Robles, M. Adaptive non-
283 local means denoising of MR images with spatially varying noise levels. *J. Magn. Reson.*
284 *Imaging* **31**, 192–203 (2010).
- 285 25. Dahnke, R., Yotter, R. A. & Gaser, C. Cortical thickness and central surface estimation.
286 *Neuroimage* **65**, 336–348 (2013).
- 287 26. Kassambara, A. & Mundt, F. factoextra: Extract and Visualize the Results of Multivariate
288 Data Analyses. R package version 1.0.7 (2020). Available at: [https://cran.r-](https://cran.r-project.org/package=factoextra)
289 [project.org/package=factoextra](https://cran.r-project.org/package=factoextra).

290

291

Supplementary Methods

292

Codes and Data Accessibility

293

294

295

296

297

298

Our sample size, hypotheses and analyses plan were pre-registered on the Open Science Framework (OSF), soon after data collection began, but prior to completion of the data collection and data analysis (project page: <https://osf.io/wu37z/>; preregistration: <https://osf.io/k6xhn>). All behavioral processed imaging data along with the analysis codes are shared on the OSF project page. Uncorrected and small-volume corrected statistical maps of the voxel-based results described in the current work are available at <https://neurovault.org/collections/8591/>.

299

Participants

300

301

302

303

304

305

306

307

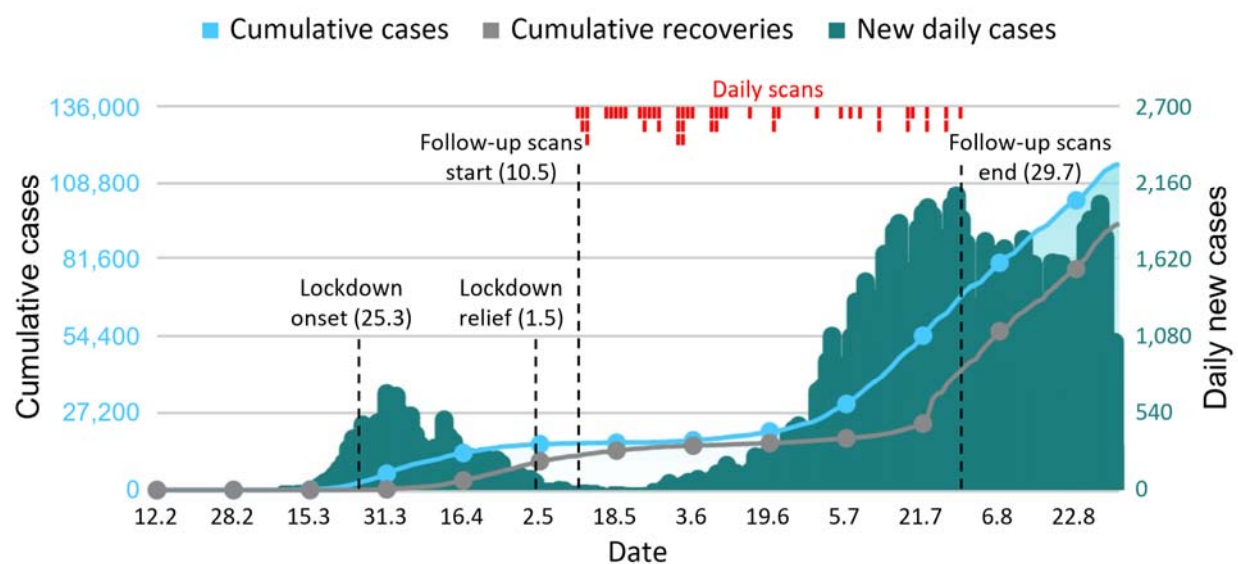
308

309

310

The study included two groups: A test group scanned before and after COVID-19 lockdown, and a control group, scanned twice before COVID-19 lockdown. All participants had no background of neurological disorders, did not show symptoms for COVID-19 and were not diagnosed as carriers of the virus. The study was approved by the ethics committee of Tel Aviv University and institutional review board (IRB) at the Sheba Tel-Hashomer medical center. Since the IRB protocol allowed us to scan the participants several times over a long period of time, we were able to collect the data from participants who were scanned prior to COVID-19 outbreak and invite them back for a follow-up scan as part of the longitudinal study they have agreed to take part in. Participants received monetary compensation for their time and gave their informed consent to take part in a longitudinal experiment aimed to examine brain plasticity across several sessions, which was initially not directly related to COVID-19 outbreak.

311 The test group comprised of $n = 50$ participants who were scanned before and after COVID-19
312 lockdown (Δ Time between scans: $M = 309.3$, $SD = 207.5$, range = 67 - 1460 days; Age: $M =$
313 30.1, $SD = 6.65$, range = 21 - 48; Females: $n = 20$, prop. = 40%). The lockdown period began on
314 March 25th, and was gradually relieved throughout late April. We mark here May 1st as the
315 lockdown relief date, as on this day an issued 100-meters movement limit for non-essential needs
316 was lifted. The test group data collection started as soon as lockdown relief took place, for a
317 period of approximately 3 months, until the end of July, 2020 (Δ Time from lockdown relief: M
318 = 57, $SD = 24.62$, range = 9 - 89 days; see Supplementary figure 1 for the study timeline).
319



320
321 **Supplementary Figure 1.** Study timeline and outbreak data

322 On February 21st, 2020, the first COVID-19 case in Israel was recorded. Daily new cases are
323 presented on green bars (right y-axis), along with the cumulative number of cases and recoveries
324 (left y-axis). Data was retrieved and modified based on the Israeli Ministry of Health reports²². A
325 lockdown was issued on March 25th, which was gradually released until the removal of the 100-
326 meter restriction on May 1st, marking lockdown onset and relief, respectively (shorter vertical
327 dashed line). MRI data of the test group was collected from May 10th to July 29th (longer vertical
328 dashed line). Red bars on top represent the number of participants scanned for the study each
329 day.

330

331 As a control group, we used the data of $n = 50$ participants who were scanned twice using a
332 similar protocol before COVID-19 lockdown (Δ Time between scans: $M = 126.7$, $SD = 190.4$,
333 range = 21 - 886 days; Age: $M = 27.3$, $SD = 5.63$, range = 19 - 42; Females: $n = 23$, prop. =
334 46%).

335 The minimal sample size was determined and pre-registered (<https://osf.io/uktsn>), based on a
336 80% power analysis conducted using R ‘pwr’ package²³, on a pilot study with $N = 16$
337 participants ($n = 8$ in each group). We decided to collect a minimum of $n = 37$ participants which
338 should provide 80% to detect the group and session interaction effect with $\alpha = .05$, within both
339 the left and right Amygdala. We originally committed to collect $n = 37$ participants in each
340 group, under the assumption it would be difficult to complete the sample due to COVID-19
341 limitations. Eventually, thanks to further relief in COVID-19 restrictions, we were able to extend
342 the sample size to $n = 50$ in each group.

343 The results remain generally consistent, even when the data included only the first $n = 37$
344 participant; demonstrating significant effects in the bilateral amygdalae, putamen,
345 parahippocampal gyrus and the left anterior temporal lobe. In this smaller sample, we did not
346 find significant effects in the right anterior temporal lobe, nor in the fusiform gyrus. We also
347 found volumetric increase effects that were not identified using the full sample in the left nucleus
348 accumbens, left cuneus, and left insula.

349 **Imaging data**

350 **Acquisition protocol.** Imaging data were acquired using a 3T Siemens Prisma scanner, with a
351 64-channel head coil. For the structural data, T1w high resolution (1-mm^3) whole brain images
352 were acquired with a magnetization prepared rapid gradient echo (MPRAGE) pulse sequence
353 with repetition time (TR) of 2.53s, echo time (TE) of 2.88ms, flip angle (FA) = 7° , field-of-view
354 (FOV) = $224 \times 224 \times 208$ mm, resolution = $1 \times 1 \times 1$. (see below).

355 Some participants were also scanned with diffusion-weighted echo-planar imaging (DW EPI)
356 sequence and some with functional gradient-echo EPI (GE EPI) in a resting state scan. The
357 analyses of these scans are beyond the scope of the current study.

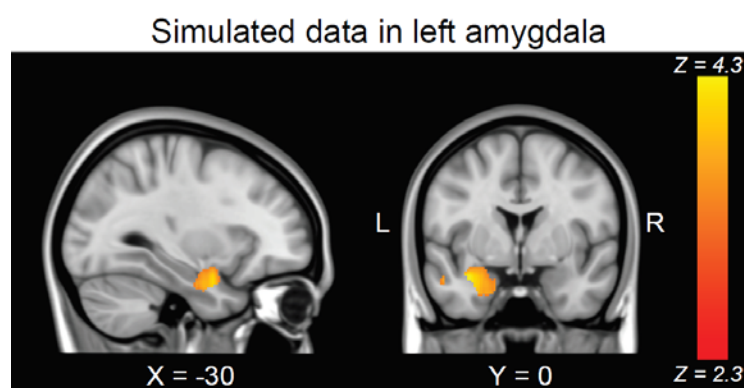
358 **Data processing and analysis.** The T1w MPRAGE anatomical scans were used for a surface-
359 based morphometry (SBM) analysis. From the images we estimated the pial and inner surfaces
360 of the cortex and projected those into the Hammers atlas (Hammers et al., 2003). Data were
361 preprocessed in SPM12 (<http://www.fil.ion.ucl.ac.uk/spm/software/spm12/>, Wellcome Trust
362 Centre for Neuroimaging) and SPM based CAT12 (Computational Anatomy Toolbox 12;
363 <http://www.neuro.uni-jena.de/cat/>, University of Jena) extension. We deployed the CAT12
364 surface-processing pipeline, which includes skull stripping, a denoising filter²⁴ projection-based
365 thickness estimation²⁵, partial volume correction, and spatial normalization to MNI space.

366 Surface-based volumetric data of cortical and subcortical regions were segmented based on the
367 Hammers Atlas, segmenting the volumetric data into 58 anatomically defined regions. Ten
368 additional ROIs of non-gray matter (ventricles, white matter, brain-stem and cerebellum ROIs)
369 were excluded from statistical analyses. To evaluate the effect of lockdown on volumetric
370 imaging data we ran a mixed linear model on the data within each one of the 58 anatomical
371 regions, examining the effect of session (baseline versus follow-up scan) and group interaction
372 (test versus control), controlling for time between scans (TBS) and time following lockdown
373 (TFL) covariates. Both covariates were mean centered before they were added to the model.
374 To identify our regions of interest we included only regions that showed both a significant
375 interaction effect (i.e. the volumetric difference between the two sessions was significantly
376 different for the test and control group), and a significant session effect within the test group (i.e.
377 a significant difference between the two sessions for the test group). Results were corrected for
378 multiple comparisons using the false discovery rate (FDR) correction, based on the number of
379 brain regions tested²¹. Following the analysis pipeline, we identified ten significant ROIs:
380 bilateral amygdalae, putamen, parahippocampal gyrus, the medial part of the anterior temporal
381 lobe, and the fusiform gyrus.
382 An additional ROI of the right inferior and middle temporal gyri showed a significant interaction
383 effect (interaction estimate = 0.17, 95% CI = [0.05, 0.29], $p = 6.1E^{-3}$, $p_{adj.} = 0.035$), however
384 examining the test group separately, we could not identify a significant session effect (session
385 estimate = 0.04, 95% CI = [-0.02, 0.10], $p = 0.259$, $p_{adj.} = 0.424$). Therefore, it is harder to
386 interpret that this interaction effect stemmed from the test group. Thus, we did not include this
387 ROI as one of our significant ROIs. A less robust session effect within the test group was also
388 observed for the left parahippocampal gyrus (session estimate = 0.04 [0.00, 0.08], $p = 0.029$, $p_{adj.}$
389 = 0.085) and right fusiform gyrus ROI (session estimate = 0.05 [0.00, 0.10], $p = 0.044$, $p_{adj.} =$
390 0.111), however as these ROIs demonstrated strong interaction effects and their session effects
391 were significant before FDR correction, we decided to report them together with the other
392 significant regions. A similar procedure was used in the pre-registration (i.e. including only
393 regions that showed a significant interaction and an effect in the test group), however in the
394 analysis of the pilot for the pre-registration, we used uncorrected results due to the small sample
395 size.

396 To examine the spatial distribution of our effect within significant ROIs, that were identified
397 with the SBM analysis, we performed an additional post-hoc voxel-based analysis. We projected
398 the data on a voxel-based map, effectively examining which voxels demonstrated an interaction
399 effect. Then, we used anatomical masks of ROIs which were found to be significant in the SBM
400 analysis, to visualize the results within these regions, similarly to a small-volume correction
401 analysis (Figure 2a)

402 **Pipeline validation**

403 To validate the imaging processing protocol we used two approaches, before data collection was
404 completed (at the time of the pre-registration finalization). As many surface-based software
405 focus on analysis of cortical surfaces, rather than subcortical regions, we aimed to validate that
406 our SBM protocol using CAT12 could reliably identify subcortical morphological changes, such
407 as the ones we observed in the current study within the amygdala and putamen. To test the
408 detection capabilities of our protocol, we generated simulated data with volumetric changes in
409 the amygdala and ran the pipeline on the simulated data. A volumetric increase in the amygdala
410 was simulated using a hand-drawn polygon mask, surrounding the left amygdala on the original
411 T1w images. Within this polygon 3D mask, the signal intensity was artificially changed.
412 Following this procedure, both the original and modified T1w images underwent the same
413 CAT12 pipeline. The analysis was performed on 10 participants. We were able to identify the
414 simulated volumetric changes within the subcortical amygdala nuclei (see supplementary Figure
415 2).



416 **Supplementary figure 2. Data simulation**

418 Sub-cortical changes in the left amygdala were simulated in ten participants. The SBM pipeline
419 applied in CAT12 identified the simulated change effect. Data was projected from surfaces back
420 to a voxel-based map for visualization in the current figure.

422 In an additional validation procedure, we reanalyzed our results with an additional analysis
423 pipeline. Raw T1-weighted maps were preprocessed using FreeSurfer. Using this alternative
424 analysis pipeline, we found similar results, including robust effects on the temporal cortical
425 regions in addition to other cortical regions. It should be noted that the FreeSurfer pipeline
426 analyze only cortical surface, thus the analysis did not include subcortical regions of the
427 amygdala and putamen.

428 The results of both validations indicated our analysis pipeline could reliably identify regional
429 volumetric estimations. Using CAT12 provided an advantage by performing a longitudinal
430 analysis of subcortical regions, including the amygdala which was pre-hypothesized and of great
431 importance in the current work.

432 **Behavioral data**

433 **Data collection.** To evaluate participants' experience in the peak days of the COVID-19
434 outbreak, we asked them to fill out a 7-items questionnaire regarding their experience of the
435 COVID-19 lockdown (see supplementary Table 1 for a description of the items). The
436 questionnaires were filled out soon after the initiation of the study, when the lockdown's
437 stringent 100-meters limitation was lifted. Most participants filled out the questionnaire on the
438 day of the post-lockdown scan session, some filled it a few days before their second scanning
439 session. A total of $n = 77$ participants filled out the COVID-19 questionnaire and comprised the
440 potential pool of test group participants for the current study, out of which $n = 50$ were sampled
441 and scanned. One participant was scanned but did not complete the questionnaire, therefore this
442 participant's behavioral data were not used and analyses of the questionnaire were based on $n =$
443 49 valid participants.

444

445

446 **Supplementary Table 1. COVID-19 lockdown questionnaire**

Question	Possible Answers (prop.)	Binary outcome (prop.)
1. Did you stay home during the lockdown, except for essential needs / did not leave at all?	0 - no 1 - yes	0 - no (20.4%) 1 - yes (79.6%)
2. Did the lockdown increase your feeling of anxiety?	0 - no 1 - yes	0 - no (61.2%) 1 - yes (39.8%)
3. With how many people did you meet during the lockdown (including people you are living with at home)?	0 - none 1 - up to three people 2 - up to five people 3 - up to ten people	0 - up to three (79.6%) 1 - more (20.4%)
4. Do you think your behavior will change following the lockdown?	0 - no 1 - yes	0 - no (65.3%) 1 - yes (34.7%)
5. How did your meeting with your parents' routine look like during the lockdown?	0 - same as before the lockdown 1 - with precaution measurements: distancing, mask, etc. 2 - did not visit at all	0 - as before or with precautions (44.9%) 1 - did not visit (55.1%)
6. What was your employment status during the lockdown?	0 - same as before lockdown 1 - full time working from home 2 - part time working from home 3 - Furlough / unemployed	0 - unemployed / part time (42.9%) 1 - same as before / full time from home (57.1%)
7. How concerned are you with the long-term effect of the lockdown, regarding yourself?	1 - 5 scale	0 - low, score 1-2 (53.1%) 1 - moderate-high, score 3-5 (46.9%)

447

448 **Data analysis.** Responses to the lockdown questionnaire were coded into binary responses,
 449 based on the sample median, splitting the sample into relatively similar sized groups for each
 450 item. To identify the main themes in the questionnaire which could be correlated with the
 451 imaging data, we performed a PCA analysis on the binarized data, using the “factoextra” R
 452 package²⁶. We found two principal components, which explained 42.6% of the variance in the
 453 sample data. These two components were extracted and correlated with the change in gray matter
 454 volumetric data in our regions of interest.

455

Supplementary results

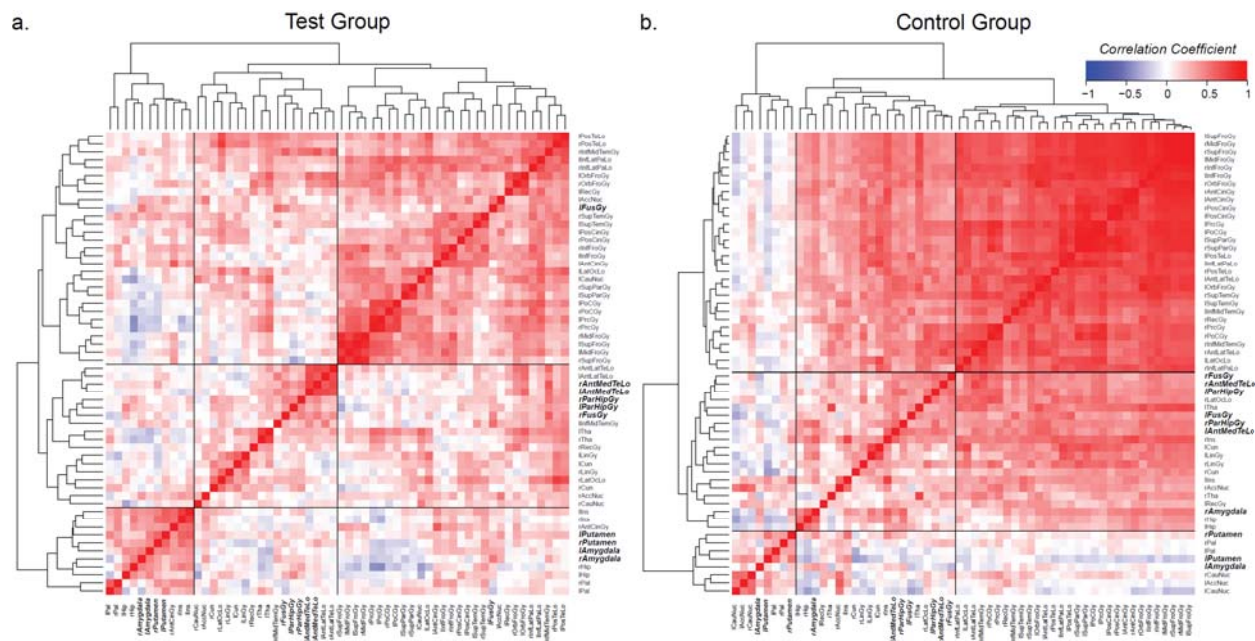
456 As an exploratory analysis, we examined whether the volumetric brain changes were associated
457 with the psychological constructs identified in our PCA analysis, based on participants' self-
458 reports. We used two linear models aimed to explain the variability in each of the principal
459 components, using the volumetric changes as our model features. Overall neither one of the two
460 PCs were well associated with the volumetric changes (Principal component 1 model: $R^2 =$
461 0.205 , $F(10,38) = 0.98$, $p = 0.475$; Principal component 2 model: $R^2 = 0.33$, $F(10,38) = 1.89$, $p =$
462 0.077).

463 While we did find some sporadic ROIs showing significant contribution within the models
464 (measured as the significance of the ROI's β estimates), after FDR correction by the number of
465 features in the model, none of the ROIs demonstrated a significant association with the PCs ($p_{adj.}$
466 > 0.05).

467 Finally, we examined correlation patterns of the volumetric change for all brain regions aiming
468 to identify shared change patterns across multiple ROIs. Hierarchical clustering of the correlation
469 matrices revealed different patterns between the two groups (Supplementary figure 3). In the test
470 group, three principal groups of clusters could be identified - the first included the palladium,
471 hippocampus, amygdala, putamen, insula (all bilaterally), and right anterior cingulate cortex, the
472 second cluster included mostly occipito-temporal cortical and subcortical nuclei, and the third
473 included highly correlated regions of the frontal, parietal and occipital cortices. All regions that
474 passed the statistical threshold of the SBM analysis (Table 1), except for the left fusiform gyrus,
475 were grouped closely together within the first two clusters, and showed low to negative
476 correlations the ROIs of the third cluster. This analysis could suggest that the origin of the
477 volumetric change observed in the regions of the two clusters might be different. The regions
478 that appear in cluster 1 are often reported in the studies that explore brain changes following
479 stress, anxiety or traumatic events⁵⁻⁸, while the regions of the second cluster are less associated
480 with specific phenomena.

481 A different pattern was observed in the control group, where the correlation pattern demonstrated
482 stronger volumetric synchrony, (Supplementary figure 3b). This could suggest that changes in
483 the control group were much more affected by within-participant effects, rather than an
484 exogenous effect (which could be the outbreak and lockdown in the test-group). It is important to
485 note in this context that in addition to the experience of the lockdown, the participants in the test
486 group also had longer time gaps between the two scanning sessions, which might provide an

487 alternative explanation for the stronger homogeneity in volumetric changes within the control
 488 group.
 489



490
 491 **Supplementary figure** . Volumetric changes correlation matrices
 492 Correlation coefficients were calculated between the volumetric change values for all ROI pairs,
 493 analyzed separately for the test (a) and the control group (b), clustered according to Euclidean
 494 distances into dendrograms. In the test group, the first and second cluster contained the
 495 subcortical nuclei (amygdala and putamen) and temporal ROI which were found significant in
 496 the SBM interaction analysis, respectively (highlighted in italic bold font). In the control group, a
 497 more homogeneous change pattern was observed with more robust correlation coefficients
 498 between the ROIs. Pearson correlation coefficients are represented by the color scheme.